RSC Advances

ROYAL SOCIETY OF CHEMISTRY

www.rsc.org/advances

The Impact of Lignin Source on its Self-Assembly in Solution

Dilru R. Ratnaweera[1], Dipendu Saha[2], Sai Venkatesh Pingali[3], Nicole Labbé[5], Amit K. Naskar[2], Mark Dadmun[1,4]

[1]Department of Chemistry, University of Tennessee, Knoxville, TN 37996, USA

[2]Material Science & Technology Division, [3]Biology and Soft Matter Division and [4]Chemical Sciences Division, Oak Ridge National Laboratory, Oak Ridge, TN 37831, USA

[5]Center for Renewable Carbon, The University of Tennessee Institute of Agriculture, Knoxville, TN 37996

Abstract

Recently, there has been a growing interest in developing value added uses for lignin, including the utilization of lignins as a precursor for carbon materials. Proper understanding of the association behavior of lignins during solution processing provides important structural information that is needed to rationally optimize the use of lignins in industry in a range of value added applications. In these experiments, we follow the assembly of lignin molecules from a variety of sources in dimethyl sulfoxide, a good solvent for lignins, using small angle neutron scattering. In order to mimic industrial processing conditions, concentrations of lignins were kept above the overlap concentration. At small length scales, short lignin segments with ~4-10 monolignol units associate to form rigid rod-like/cylindrical building blocks, where the number of repeat units in a cylindrical segment decreases with increasing lignin concentration. These cylindrical building blocks associate to form aggregates with low cross-linking densities and a

random coil or network like structures from highly branched lignin structures. The degree of branching of the base lignin molecule, which varies with source, plays a crucial role in determining their association behavior. The overall sizes of the aggregates decrease with increasing concentration at low cross-linking densities, whereas the opposite trend is observed for highly branched lignins.

Introduction

Lignin, a three dimensional network of cross-linked phenylpropanoid subunits that exists in plant cell walls, is one of the most naturally abundant organic polymers, second only to cellulose in natural abundance.[1-2] Even though large quantities of lignin are produced every year as a byproduct of biofuels and papermaking processes, lignin has a limited market. It is primarily used in low value applications such as a combustion fuel.[3] Recently, there has been a growing interest in utilization of lignins as fillers for polymer or as a precursor for carbon fibers, owing to their low cost and availability.[4-8] However, its low molecular weight, poor thermal stability, wide variation in time and temperature dependent melt-viscosity, and a limited knowledge of precise lignin architecture limit its ability to compete with synthetic polymers.[1]

The structure of lignin is formed by oxidative coupling of 4-hydroxyphenylpropanoid monomers in plants.[8] There are three major monolignol units in lignin; coniferyl alcohol, sinapyl alcohol, and *p*-coumaryl alcohol (Figure 1). [8] The monolignol composition of lignin varies from one plant source to another, further complicating the use of lignin in targeted value added applications. For instance, hardwood lignins have more sinapyl alcohol and softwood lignins have more coniferyl monolignols. The differences in monolignol composition and the randomness of oxidative coupling results in high polydispersity of molecular weight and

structure in lignin molecules. [9-10] The molecular weight distribution of an extracted lignin also depends on the type of isolation technique (kraft, solvent extraction, soda, sulfite, etc.) that is used to extract the lignin from the ligno-cellulosic biomass.[11-13] In addition to the limited knowledge of the chemical and physical properties of lignin, there is limited information available that defines the association behavior in solution, which depends on the solvent conditions and lignin structure.

Lignins tend to aggregate in most solvents, and this aggregation significantly impacts the isolation of lignins from plants, as well as the preparation of lignin based advanced materials. Because of the importance of lignin solution behavior in both these processes, the association of lignin molecules in different solvent conditions has been investigated for the last several decades.[9, 10, 14] These results indicate that even though they are low molecular weight compounds, lignins aggregate in most solvents at low concentrations.[15] The size and molecular weight of these aggregates vary depending on the solvent quality, the monolignol composition, ionic strength and temperature.[14] Extracted lignins have been reported to consist of only a few monolignol units and the average degree of polymerization is mostly less than 10 (thus these molecules are oligomers).[16]

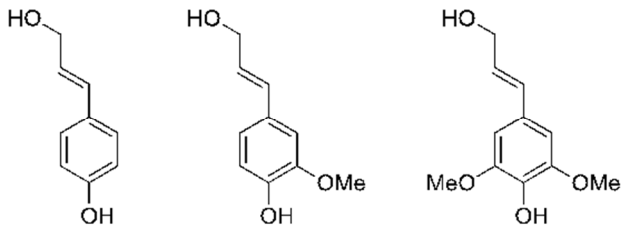

p-coumaryl coniferyl sinapyl alcohol

Figure 1. Chemical structure of basic monolignol units, p-coumaryl alcohol, coniferyl alcohol and sinapyl alcohol

These lignin aggregates are thermally stable and form by cohesive interactions among lignin molecules, which can be weakened by deprotonizing acid (phenolic and carboxylic)

groups or by ionic liquids. Some studies have shown that intermolecular hydrogen bonding dominates the formation of lignin aggregates and other studies have illustrated the importance of the π- π stacking of aromatic groups on their association in solution. Such π- π associations can be suppressed by the presence of lignin complexing agents such as iodine, which weaken π- π interactions.[15] In alkaline solutions, lignins adopt expanded aggregates.[14, 17] For instance, Cheng *et. al.* have shown that lignins in aqueous solutions consist of well defined elongated nanometer scale subunits, which expand significantly in alkaline solutions at lower concentrations.[18] They interpret their results to indicate that these subunits associate to form a three-dimensional network of lignins. Additionally, Petridis and coworkers have used SANS and molecular dynamic simulations to study the structure of softwood lignins dispersed in water.[19] They have observed fractal aggregates with highly folded surfaces. SANS studies have shown that these lignin assemblies deviate from their linear structure in solutions.[20] The architecture of the extracted lignins is somewhat rigid and those molecules assemble into shapes that vary from nanogels to heavily branched structures. The formation of a sol or gel of lignin molecules is due to the absence or presence of intermolecular interactions between functional groups (such as hydroxy, ether and carboxylic) of neighboring lignin molecules.[21-22]

Understanding the assembly of lignin molecules in solution is crucial as the heterogeneity in the structure of lignin and the unknown molecular characteristics of the available lignin has presented obstacles in converting these abundant resources to useful renewable materials.[23] One can draw an analogy to polymeric materials, which exhibit significantly different properties with a variation in molecular architecture.[24] A straightforward example is the impact of branching on the behavior of polyethylenes, where linear high-density polyethylene (HDPE) is highly crystalline while the highly branched low-density polyethylene (LDPE) is not. These differences

in molecular structure translate to a dramatic improvement in impact strength and modulus of HDPE relative to that of LDPE. Therefore, understanding the assembly and molecular architecture of lignin, and correlating this structure to its molecular composition and source, is crucial for the development of value added materials from lignin.

Moreover, one can treat the structure of lignin in solution in a similar manner to other polymers connected by crosslinks. Compared to linear polymers, highly cross-linked polymers have a three dimensional network-like structure in good solvent conditions.[25] In general, the assembly of polymers in solution depends on the polymer-polymer and polymer-solvent interactions, molecular weight, chain architecture, concentration and temperature.[26-28] The shapes and sizes of these aggregates are governed by the free energy of the solutions, where molecules arrange to minimize the free energy of the system. Minimization of free energy during the self-assembly process is achieved by overcoming unfavorable change in entropy (ΔS) with favorable enthalpic interactions (ΔH) that guide the assembly of molecules.[29] However, a simple model to describe the solution structure of all lignins may not be possible due to differences in monolignol composition, associated conformations, and branching among lignins that are isolated from a variety of sources.

Previous extensive studies on the hierarchical structure of branched polymers can be leveraged to model lignin aggregates as a branched polymer. Previous studies have shown that the hierarchical structure of branched polymers depends strongly on the cross-linking density[25], where, for lignins, the cross-linking density depends on the number of methoxy groups in the monolignols, as oxidative coupling takes place through these segments. Given that the composition of the monolignols in a lignin varies from one source to another, different molecular structures and aggregation behavior is not unexpected for lignins derived from different original

plants. Given this complexity, a clear picture of the association of lignins and its correlation to the precise structure of the lignin as defined by its source is not clear. With this in mind, we have studied the solution structure of lignins from different sources, and therefore consisting of different cross-linking densities in dimethyl sulfoxide (DMSO) using small angle neutron scattering (SANS). Contrast variation between the lignin and deuterated solvent provides sufficient scattering to accurately characterize the solution structure of lignin samples with different methoxy group densities obtained from different plants. The lignin concentrations studied in this work are comparably higher than other reports in the literature, because these concentrations are in the range of industrial processing conditions.

Experimental Section

Material

Three types of lignins were studied in this work ─ Kraft processed softwood lignin, organosolv extracted hardwood lignin, and acid extracted lignin from wheat straw. Usually softwood lignin has high coniferyl alcohol content, hardwood has high sinapyl alcohol content, and coumaryl alcohol dominates in wheat straw lignin. Thus, depending on the source, lignins used in this study have different methoxy group densities.

The chemical composition of the lignin samples was determined by following procedures developed by the National Renewable Energy Laboratory (NREL/TP-510-42618 and NREL/TP-510-42622)[37]. In brief, around 300 mg lignin sample went through a two-step acid hydrolysis and separated into soluble and insoluble fractions by filtration. The acid soluble lignin content was measured using a UV-Vis spectrophotometer (Thermo Scientific GENESYS 10S). The mono-sugar content of polysaccharide was quantified using a High Performance Liquid Chromatograph

(Perkin Elmer 200 series) equipped with an Aminex HPX-87P column (Bio-Rad). The acid insoluble lignin was calculated by gravimetric method. The ash content of the lignin was determined gravimetrically after combustion of the non-ash material at 575 °C for 24 h in a muffle furnace (Fisher Scientific). The sulfur content was measured after acid digestion by inductively coupled plasma-optical emission spectroscopy (ICP-OES, Optima 7300. Perkin Elmer). To complete these analyses, all lignin samples were ball milled for 30 seconds, then the fine powders were loaded into a Frontier EGA/Py-3030D pyrolyzer connected to a Perkin Elmer Clarus 680 Gas Chromatography and SQ 8C Mass Spectrometer system for structural characterization. Each sample was pyrolyzed for 12s at 450 °C. Syringyl to guaiacyl ratio of each lignin was determined following the method described by Sykes et al.[38] For efficient separation of the components the GC oven temperature was held at 50 °C for 4 minutes, then heated to 270^{o}C at 5^{o}C/min (total 40 minutes). A Perkin Elmer Clarus SQ 8C Mass Spectrometer was used for the identification of the separated compounds. Mass scan was performed from *m/z* 35 to 550. Ion source temperature for MS was 270^{o}C and electron ionization was 70 eV. NIST library and the literature data were employed for the purpose of matching the mass spectral fragmentation pattern to identify the evolved products and to assign the corresponding lignin fragments (syringyl and guaiacyl units). Syringyl to guaiacyl ratio was estimated following the method described by Sykes et al.[38] The area values of the syringyl peaks with *m/z* 154, 168, 182, 194, 208 and 210 were summed and divided by the sum of guaiacyl peaks with *m/z* 124, 138, 150, 164 and 178.

The physical characteristics of the lignins that are studied in these experiments are shown in Table 1. In the scattering experiments, the lignins were dissolved in deuterated DMSO to obtain 5, 10 and 15 wt./vol% solutions. 15 wt./vol% was the highest concentration studied as this

approaches the solubility limit of the highly cross-linked wheat-straw derived lignin. Table 1 also shows the glass transition temperatures (T_g) and hydroxyl group content of the isolated lignins studied in this work. The as-received organic acid extracted wheat straw lignin is a partially esterified derivative and has the least hydroxyl group content. The molecular weight data of the hardwood and wheat straw lignin used in this study (shown in Table 1) were obtained on acetylated derivatives, as such modified lignins do not exhibit extensive hydrogen bonding or agglomeration. For the softwood lignin to avoid agglomeration in dimethyl formamide, LiBr salt (0.05 M) was used and corresponding molecular weight data are shown in table 2. All lignins studied in these scattering experiments are oligomeric in nature with number average molecular weight ranging from 1000 Da to 2360 Da and polydispersity index (PDI) varies from 1 to 3.

Table 1. Characteristics of lignin samples

Lignin sample	**Source**	**Molecular weight (M_n)**	**PDI**	**T_g (°C)**	**Total hydroxyl group content [phenolic, aliphatic, carboxylic] (mmol/g)**
Kraft processed softwood lignin	Kruger Wayagamack Inc. Canada	2360 [30]	3.1	153	5.1 [3.4, 1.7, 0.0] [30]
Organosolv processed hardwood lignin	Lignol Innovations, Canada	1000 [20]	3.0	99	5.6 [4.0, 1.5, 0.1] [31]
Organic acid extracted wheat straw Biolignin™	CIMV, France	1634 [32]	1.3	172	4.9 [1.0, 3.9, -] [32]

Small Angle Neutron Scattering

Small angle neutron scattering (SANS) experiments were completed on the CG-3 Bio SANS at Oak Ridge National Laboratory. A discussion of the capabilities and limitations of small angle neutron scattering is provided in the supplemental information for the interested

reader. The data were collected at three different instrument configurations to determine the scattering of the solutions over a *q* range of 0.003 – 0.7 $Å^{-1}$, where q is the momentum transfer, given by $q=4\pi\sin(\theta)/\lambda$, where θ is the angle of incidence, and the neutron wavelength (λ) is 6 Å. Sample to detector distances were 14.5, 6 and 0.3 m to obtain data from *q* ranges of 0.003 – 0.067 $Å^{-1}$, 0.0067 – 0.0914 $Å^{-1}$ and 0.057 – 0.67 $Å^{-1}$ respectively. The resolution of the instrument ($\Delta\lambda/\lambda$) is 0.15. Data reduction was carried out using the KCL SANS package developed at ORNL. The scattering from background, empty cell and deuterated DMSO were subtracted from the data and the data were corrected for the transmission of individual samples. SANS data were analyzed using SANS software packages developed at NCNR NIST. In these analyses, the scattering length density (SLD) values of 1.26×10^{-6} $Å^{-2}$ for lignin and 5.28×10^{-6} $Å^{-2}$ for deuterated DMSO were used as initial parameters during data analysis.

The low *q* data of all samples and the full *q* range of the wheat straw lignin solutions were analyzed using the multi-level unified exponential/power law model (Equation 1), which is a combination of Guinier and Power laws, developed by Beaucage *et al*. [33]

$$I(q) = \sum_{i=1}^{N} G_i \exp\left(-\frac{q^2 R_g^2}{3}\right) + \frac{B_i\left[erf(qR_{g,i}/\sqrt{6})\right]^{3P_i}}{q^{Pi}} + Bkg \qquad (1)$$

In this equation, *G* is the Guinier pre-factor, *B* is the pre-factor of power law scattering, P_i is the power law exponent and R_g is the radius of gyration. R_g of the aggregates obtained from the Guinier law is independent of the shape of the aggregates and the value of the scattering at *q* = 0. *B* is normally defined according to the power law regime or with the regime that provides P_i. The value of P_i provides information about the shape of the scattering objects and its fractal

structure. The high q data of some lignins were modeled using cylindrical form factor ($P(q)$), which is shown in Equation 2.[34]

$$P(q) = \frac{Scale}{V_{Cyl}} \int_0^{\pi/2} f^2(q,\alpha) \sin\alpha d\alpha \qquad (2)$$

$$f(q,\alpha) = 2(\rho_{cyl} - \rho_{solv}) V_{cyl}\, j_0(qH\cos\alpha) \frac{J_1(qr\sin\alpha)}{(qr\sin\alpha)}$$

$$j_0(x) = \sin(x)/x$$

In this equation, V_{cyl} is the volume of the cylinder, $J_1(x)$ is the first order Bessel function, α is the angle between cylinder axis and the scattering vector, H equals half of the length of the cylinder, and ρ_{cyl} and ρ_{sol} are the SLDs of the cylindrical scattering object and the solvent surrounding it.

Results and Discussion

Lignin samples selected for this study were obtained from various plants, which have different monolignol compositions, therefore different cross-linking densities. The SANS data of hardwood lignin, which has the highest methoxy content (and presumably lowest cross-link density), dissolved in d-DMSO are shown in Figure 2a. The data are shifted vertically for clarity, but the 5 wt./vol.% data are in absolute intensity units (cm^{-1}). The low q upturns were observed for all lignin concentrations, indicating the presence of large scattering objects due to the association of lignin molecules. The shape of the scattering patterns at high q (above 0.015 $Å^{-1}$) hardly changes and only the slopes at low q change with lignin concentration. This indicates that the building blocks of the aggregates at small length scales are similar for all lignin solutions;

only the association processes of the building blocks into the aggregates is affected by the concentration or lignin type.

In order to estimate the shape of the scattering objects at different lengths scales, the slopes of the log-log plots of the SANS data at different q ranges were analyzed. The slopes at low q (below 0.015 $Å^{-1}$) are about 4 and they slightly decrease with increasing concentration. This indicates that at larger length scales, the scattering is dominated by large aggregates. The slopes at high q (above 0.1 $Å^{-1}$) are about 1, which corresponds to scattering from elongated/rod like objects. Figure 2c shows the Kratky representation of the hardwood SANS data, where $I(q)q^2$ is plotted as a function of q. In this plot, $I(q)q^2$ increases linearly with q at high q, which verifies the stiff chain/rod like nature of the particle at this length scale. The slopes of the log-log plots at high q are provided in Table 2.

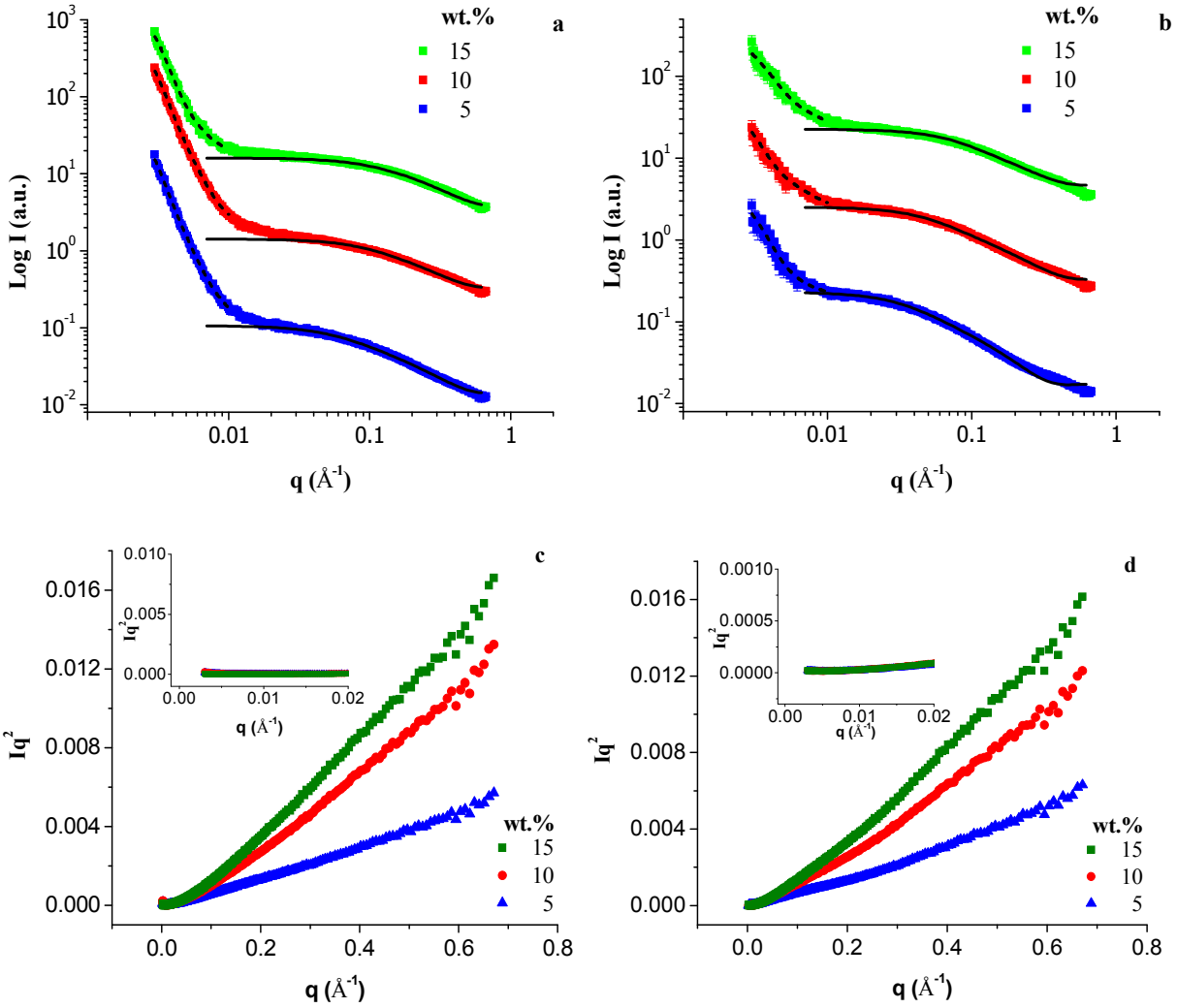

Figure 2. SANS data of **(a)** hardwood and **(b)** softwood lignins. Symbols correspond to the experimental data, solid lines are the best fits obtained for cylindrical form factor and dash lines are the modeled data using unified model. **(c)** and **(d)** are the Kratky representations of hardwood and softwood data with inset focusing on low *q* regime.

Figure 2b shows the SANS data for softwood lignin, which has less methoxy content and more potential to form branched chain structure relative to the hardwood lignin, which is consistent with the fact that the as-received hardwood lignin is melt-extrudable, while the other lignins are not. The shapes of the scattering patterns of the softwood and hardwood lignins in solution are quite similar. The crossover between the low *q* upturn and high *q* structure is shifted towards low *q* (around 0.008 Å^{-1}) for the softwood lignin, indicating that the building blocks of

the softwood lignin aggregates are comparably larger than those of the hardwood lignin aggregates. As indicated in Table 2, the low q Porod slope of 2.7 obtained for the 5 wt.% softwood lignin solution indicates that the scattering from this solution is governed by a rather dense network like structure at larger length scales that is formed by the aggregation of cylindrical/rod like shape objects. As concentration increases, the large scale (low q) structure transitions into a two dimensional object such as sheets, lamella, disks or random coils, all of which have fractal dimension of 2. At high q, cylindrical shaped objects dominate the scattering. This is confirmed by the linear increase in $I(q)q^2$ with increasing q shown in Figure 2d. Therefore, as the lignin concentration increases, the shape of the overall aggregate varies while keeping the anisotropic, cylindrical shape of the building blocks. Interestingly, the basic building blocks of the softwood and hardwood aggregates in solution have a similar elongated shape; however, aggregates of these building blocks at larger scale are denser for hardwood lignin and more open for softwood lignin.

Table 2. Log-Log slopes of the various lignin solutions at low and high q

	Low q region			**High q region**		
Concentration (wt./vol %)	**Hardwood**	**Softwood**	**Wheat Straw**	**Hardwood**	**Softwood**	**Wheat Straw**
5	-4.4	-2.7	-2.4	-0.9	-1.0	-0.8
10	-4.3	-2.0	-2.8	-0.7	-0.8	-0.8
15	-3.9	-2.0	-3.2	-0.7	-0.7	-0.7

The clear crossover between the low and high q regions (around 0.01 $Å^{-1}$) reflects that the structures at these length scales correspond to different shapes. At q values above the crossover, the data readily follow the cylindrical form factor given in Equation 2. The best fits obtained for the cylindrical form factor to the scattering data are shown as solid lines in Figures 2a and 2b for hardwood and softwood lignins, respectively. In both lignins, the minimum q that properly fit to a cylindrical form factor increases with increasing concentration, indicating that the size of the cylindrical building block decreases with concentration, or as the molecular crowding increases. The structural parameters that are derived from fitting the high q data to a cylindrical form factor are shown in Figure 3. These results show that the average radius of the cylindrical building blocks decreases with increasing lignin concentration for the softwood lignin. Moreover, the diameter of the cylindrical building blocks of the hardwood lignin aggregate is about the size of a single monolignol unit and barely changes with lignin concentration. In the softwood lignin aggregate, the diameter of these building blocks at 5 wt./vol.% is about 18 Å, which would result

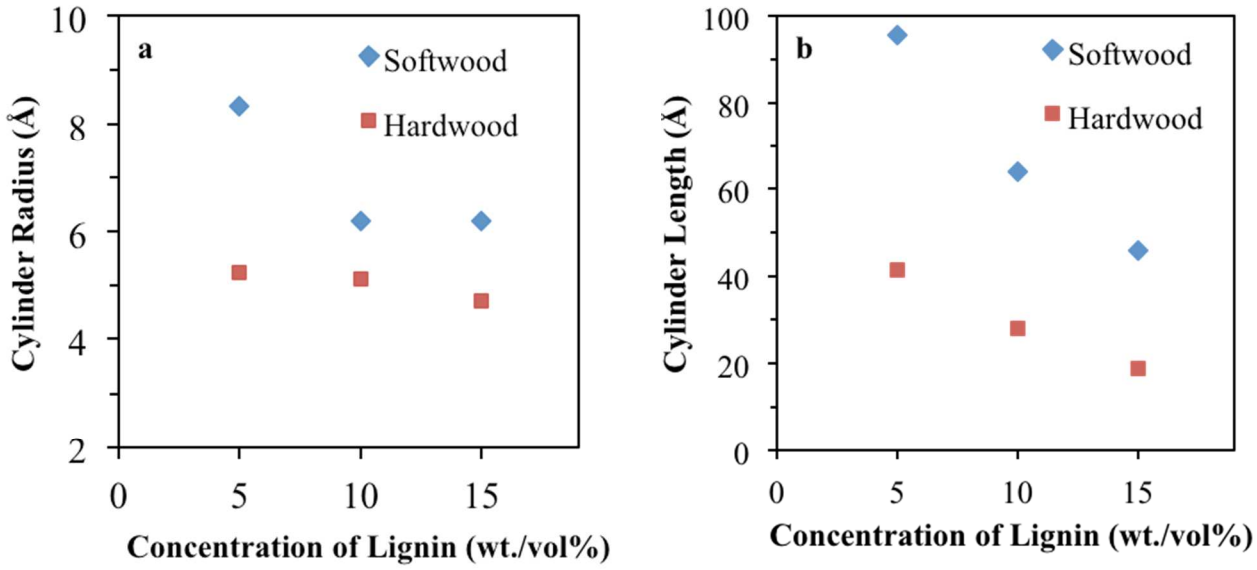

Figure 3. (a) Radii and **(b)** lengths of the hardwood and softwood lignin aggregate cylindrical building blocks as a function of concentration in dDMSO as derived from the analysis of the high q scattering pattern.

from the association of two lignin chains to form the cylindrical building block. However, at 10 and 15 wt./vol.% solutions, the cylindrical building block is similar in size to that of the hardwood lignin aggregate, suggesting a single lignin chain.

Figure 3b shows the lengths of the cylindrical building blocks as a function of concentration, demonstrating that they decrease with increasing concentration for both the hardwood and the softwood aggregates. The lengths of the cylindrical building blocks of the softwood aggregates are longer than those of the hardwood solution aggregates. These differences in lengths appear to be primarily governed by the monolignol composition of the individual lignin molecules. The different monolignols vary in the number of methoxy functional groups (Figure 1) that can interact with vinyl groups of other monolignols during lignin biosynthesis, which impacts the extent of branching in the individual lignin molecule. For instance, a lignin with many sinapyl alcohol units (such as hardwood lignin) may deviate from an elongated cylindrical shape within fewer repeat units than one with more *p*-coumaryl and coniferyl monomers (such as softwood lignin).

The differences in the sizes of the cylindrical building blocks are based on the combination of the intermolecular interactions and the excluded volume effects. When lignin concentration increases, the crowding of the molecules increases, providing an environment where further intermolecular interactions between neighboring molecules can form. These interactions can reduce the length of the elongated building blocks. However, steric hindrance resulting from the bulkiness of the phenylpropanoid units and limited flexibility of the cyclic ether groups bolsters the rigid nature of the building blocks. At high concentrations, the length scale of the shortest rigid segment is decreased due to the excluded volume interaction. These excluded volume effects are long-range interactions compared to the effect of the intermolecular

interactions. The combination of these factors appears to guide the length of the cylindrical building block to vary between 4 to 10 monolignol units. This calculated degree of polymerizations (DP) coincides with the length of linear lignin oligomers that Crestini *et al.*[16], determined by NMR of milled wood lignin.

The large-scale structure of the aggregates that is formed by the assembly of the cylindrical building blocks can be characterized by the analysis of the low *q* data. This low *q* data were analyzed using a single level unified power law and Rg model, which is a combination of a Guinier and a power law analysis. The fits of this model to the data are shown as dotted lines in Figure 2a and 2b for hardwood and softwood lignins, respectively. The slopes of the log-log plot extracted from this analysis are identical to the slopes obtained from the Porod fit (Table 2). Furthermore, this analysis provides a quantitative measure of the radius of gyration of the overall aggregates as a function of lignin concentration, which are shown in Figure 4. These results show that the aggregates of the softwood lignin are smaller than those of the hardwood lignin.

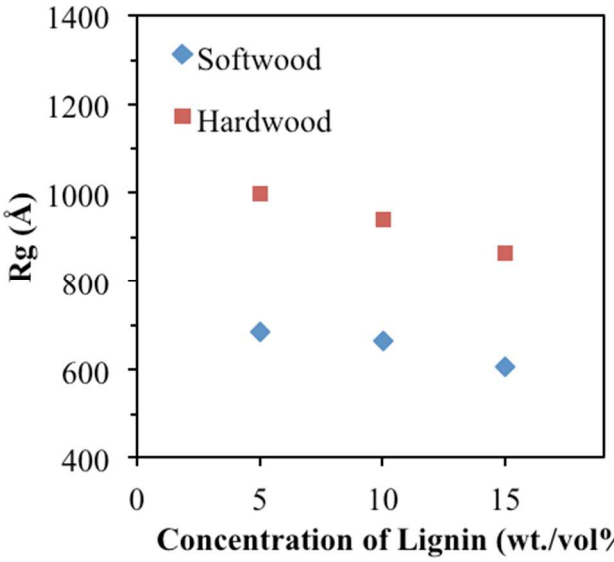

Figure 4. Radius of gyrations (R_g) of of softwood and hardwood lignin aggregates as a function of concentration in dDMSO.

Interestingly, in both softwood and hardwood lignins, the aggregate size decreases with increasing concentration. This trend can be understood as a screening of intermolecular interactions between molecules with increased concentration, which is a direct result of a decrease in distance between molecules as concentration increases.

This behavior is consistent with the results of Daoud and Cotton that have shown that the size of aggregates that branched polymers form in solution decreases with increasing polymer volume fraction (ϕ) above the overlap concentration (ϕ^*), where $R_g \sim (\phi/\ \phi^*)^{-1/8}$.[35] In these previous studies, their analysis shows that the mass concentration is the highest at the center of the branched polymer in dilute solution, where the mass concentration decreases with increasing distance from the center. Above the overlap concentration, the polymer chains from different molecules/aggregates may penetrate into the pervaded volume of the less crowded outermost chains of the branched polymer, which causes a contraction into a smaller volume. Cheng and coworkers have reported similar trends for lignins with low sulfonate content in alkaline conditions.[18] At low concentrations, the lignin molecules/aggregates are highly expanded and their sizes decrease with increasing concentration.

The SANS data of the wheat straw lignin solutions are shown in Figure 5a. Inspection of these curves clearly shows that the scattering patterns of the wheat straw lignin solutions differ significantly from those of the other two lignin solutions and do not show any clear cross-over in structure from low to high q. Since the polydispersity of this lignin is very low (Table 1) these featureless SANS curves could be a result of a high crosslink density of the wheat lignin, which is consistent with the limited presence of phenolic hydroxyl groups. The glass transition temperature of this lignin is very high (172 °C) relative to that of the hardwood and softwood lignins, which is consistent with a more crosslinked structure. Analysis of these results show that the slopes of the log-log plot at low q increase with increasing concentration from 2.4 to 3.2 indicating the transition from an open coil-like structure to more dense, network like aggregates. The slopes of the log-log plot at high q decrease with concentration but remain ~ 1, which represents elongated, rod-like scattering objects. In spite of this analysis, the high q data could

not be modeled with a cylindrical form factor as utilized in the analysis of the softwood and hardwood lignins. Therefore, a detailed characterization of the shape of the building blocks of the wheat straw lignins could not be resolved from these scattering curves. Although this lignin is randomly crosslinked, its high T_g and phenolic nature make it a useful material for use in lignin-derived polymeric materials.[36]

In order to characterize the dimensions of the overall aggregates and the building blocks, the SANS curves were analyzed using a three level unified fit model, where the fits are shown as the solid lines in Figure 5a. The Rg of the aggregates that derive from these analyses as a function of lignin concentration are shown in Figure 5b. The dimensions obtained from the medium and high *q* regions are similar to those of the cylindrical building blocks of softwood and hardwood lignins. However, the exact structure of the aggregates over this length scale is difficult to ascertain due to lack of structural feature in the SANS curves. The analysis of the large-scale structure of the aggregates shows that their size increases with concentration, which

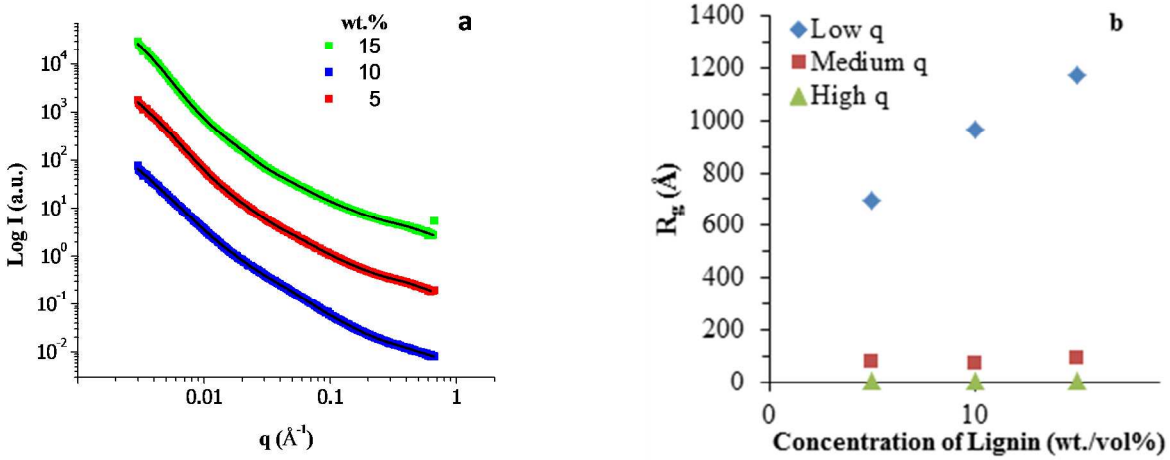

Figure 5. (a) SANS data of wheat straw lignin in dDMSO as a function of lignin concentration. Symbols correspond to data and solid lines are the best fits obtained from three level unified model. Data and fits were shifted vertically for clarity. **(b)** R_g values obtained from unified model for low, medium and high *q* regimes.

is opposite to the behaviors of softwood and hardwood lignin solutions. This may be due to the fact that the wheat straw lignin is a highly branched/cross-linked polymer. Therefore, the density of the lignin segments is higher, limiting any interpenetration of neighboring polymers. This denser packing density leads to a larger barrier to the interpenetration of neighboring chains, which results in the formation of larger clusters with increased concentration. This interpretation is also consistent with the limited solubility of this lignin in DMSO, suggesting a higher cross-linking density.

The discussion of these results has focused on the importance of the structure of the lignin as the dominant feature that controls the assembly of the lignin in solution. It may also be that impurities in the lignins, such as inorganics or additional carbohydrates, or the specific isolation process may alter the structure of the lignin, which contributes to the assembly process. To address this potential factor, we have determined the chemical composition of the lignin samples studied here, including the amount of cellulose, hemicellulose, ash, sulfur content, and the ratio of syringyl to guaiacyl content (S/G) of the lignins to investigate if there is a correlation between these features and the assembly of the lignin in solution. These characteristics of the lignins are shown in Table 3.

Inspection of the results in Table 3 clearly shows that the dominant feature that governs the assembly of the lignin in solution is the structure of the lignin. The role of impurities, inorganics, and additional carbohydrates content is secondary to the assembly. For instance, the total amount of inorganic ash from each lignin is similar and less than 1%, and thus its presence cannot be correlated to the assembly processes of the three lignins.

The amount of sulfur does vary among the three lignins, with the Kraft softwood lignin containing the greatest amount. This is not surprising as the isolation process leaves residual bound sulfur in the lignin. However, a closer examination of the correlation of the assembly of the lignins to the amount of sulfur clearly shows that the presence of the bound sulfur cannot explain the difference in assembly of the various lignins. The scattering results show that both the hardwood and softwood lignins assemble into well-defined structures from cylindrical building blocks, while the building blocks of the assembly in the wheat straw lignin are less well structured. Thus, the assemblies of the softwood and hardwood lignins are most similar to each other. However, inspection of the sulfur content shows that the hardwood lignin has the least amount of sulfur (< 200 ppm) while the softwood lignin has the most sulfur (> 13000 ppm). If the sulfur content were influencing the assembly of these two lignins, one would expect that their assembly structure and process to differ more significantly, given the extreme variation in the sulfur content.

Table 3: Structural and composition analysis of the lignins studied

Components	**Kraft processed softwood lignin**	**Organosolv processed hardwood lignin**	**Organic acid extracted wheat straw Biolignin™**
Cellulose (%)	0	0	1.20 ± 0.01
Hemicellulose (%)	1.10 ± 0.01	0.70 ± 0.01	1.90 ± 0.01
Inorganic Ash (%)	0.34 ± 0.03	0.24 ± 0.07	0.88 ± 0.03
Sulfur (mg/kg)	13,408 ± 2	176 ± 5	1441 ± 1
S/G	0.06 ± 0.01	2.63 ± 0.08	0.31 ± 0.01

The ratio of syringyl to guaiacyl of the lignin (S/G), which correlates to the chemical structure of the lignin, was also determined and does appear to correlate to the assembly of the

lignin in solution. The S/G ratio of the hardwood lignin is the largest (~2.6), while that of the softwood lignin is the smallest (~0.06), and that of the wheat straw lignin is in the middle (0.31). These values are consistent with a high guaiacyl content in the softwood lignin and high syringyl content in the hardwood lignin, where this variation is consistent with the modest changes in the assembly behavior of these two lignins as described above.

Finally, the amount of cellulose and hemicellulose remaining in each lignin, indicates that the softwood and hardwood lignins do not contain any cellulosics, but the wheat straw lignin does. Therefore any variation between the assembly of the hardwood and softwood lignin cannot be a result of the presence of cellulose or hemicellulose. However, in the wheat straw lignin, the combination of the modest S/G content, which denotes that neither structure dominates, and the approximately 3% cellulosics suggests that this sample is quite heterogenous, which is consistent with poorly defined building blocks of this material.

Therefore, all 3 types of lignin dissolved in a good solvent (DMSO) show formation of lignin aggregates with rod shaped building blocks that are about the thickness of a monolignol unit. The sizes of these rigid rods are affected by the concentration of the lignin solutions, where sizes of these building blocks decrease with increasing the lignin concentration in DMSO. Also the lengths of the building blocks are determined by the lignin polymer chain flexibility and branching. The chain flexibility can be linked to the monolignol structures present, which impacts the presence of branching or crosslinking sites in the original lignin. Monolignols with more methoxy functional groups have less tendency to form branched or crosslinked structures, relative to lignins consisting of monolignols with fewer methoxy functionalities.

The Low T_g hardwood lignin, being relatively the most flexible oligomer, forms a coiled structure with shorter building blocks, which aggregate into more dense aggregates. The intermediate T_g softwood lignin forms a longer building block, which assemble into more open, 2-dimensional aggregates at higher concentrations. The very high T_g wheat straw lignin is more highly crosslinked, and therefore does not exhibit a regular building block. This lignin forms aggregates that are also not as dense due to the steric hindrance of the crosslinked aggregates assembling, which results in an increase in aggregate size at higher concentration.

Conclusions

The current study demonstrates that the assembly of lignin molecules in solvents varies based on the source of the lignin, where the amount of methoxy groups present in the lignin, and therefore its ability to form crosslinks, guides their assembly. The aggregates formed from softwood and hardwood lignins consist of well-defined cylindrical building blocks with 4-10 monolignol units, where the number of monomers per building block is affected by lignin concentration. These building blocks arranged into large aggregates with well-defined shapes such as dense isotropic structures, network-like, random coils or two-dimensional objects depending on the source of lignin. Lignin concentrations used in this work are above the overlap concentration, hence pervaded volume of the outermost chains are overlapped with neighboring chains, which results in the decrease in aggregate size with concentration for the loosely packed aggregates formed by softwood and hardwood lignin. The more densely packed lignin, however, behave in an opposite manner, where the lignin molecules associate to form larger aggregates with increasing concentration.

Acknowledgement

This work was supported by the Department of Energy, Office of Basic Sciences, through the EPSCoR grant, DE-FG02-08ER46528 and the Laboratory Directed Research and Development Program of Oak Ridge National Laboratory, managed by UT-Battelle, LLC, for the U.S. Department of Energy under Contract No. DE-AC05-00OR22725. The authors also wish to acknowledge the Joint Institute for Neutron Sciences at the University of Tennessee for support of this project. The research at ORNL's Center for Structural Molecular Biology (FWP ERKP291) was supported by the U.S. Department of Energy's Office of Biological and Environmental Research. A portion of this research at Oak Ridge National Laboratory's High Flux Isotope Reactor was sponsored by the Scientific User Facilities Division, Office of Basic Energy Sciences, U.S. Department of Energy. The authors also acknowledge the generous donation of the lignin samples from Lignol Innovations, Canada, Kruger Wayagamack Inc. Canada, and CIMV, France.

References

1. Lora J. H., Glasser W. G., *J. Polym. Environ.*, **2002**, *10*, 39 - 48
2. Mao J. Z., Zhang L. M., Xu F., *Cellul. Chem. Technol*, **2012**, *46*, 193 - 205
3. Vainio U., Lauten R. A., Serimaa R., *Langmuir*, **2008**, *24*, 7735 - 7743
4. Huang X., *Mater.*, **2009**, *2*, 2369 – 2403
5. Baker D. A., Rials T. G., *J. Appl. Polym. Sci.*, **2013**, *130*, 713 – 728
6. Sudo K., Shimizu K., Nakashima N., Yokoyama A. *J. Appl. Polym. Sci.*, **1993**, *48*, 1485 – 1491
7. Rosas R. R., Bedia J., Lallave M., Loscertales I. G., Barrero A., Mirasol J. R., Cordero T., *Carbon*, **2010**, *48*, 696 – 705
8. Ralph J., Lundquist K., Lu F., Kim H., Brunow G., Schatz P. F., Marita J. M., Hatfield R. D., Ralph S. A., Christensen J. H., Boerjan W., *Phytochem. Rev.*, **2004**, *3*, 29 – 60
9. Contreras S., Gaspar A. R., Guerra A., Lucia A. A., Argyropoulos D. S., *Biomacromolecules*, **2008**, *9*, 3362 – 3369
10. Sarkanen S., Teller D. C., Abramowski E., McCarthy J. L., *Macromol.*, **1982**, *15*, 1098 – 1104

11. Ross K., Mazza G., *Int. J. Mol. Sci.*, **2010**, *11*, 4035 – 4050

12. Biljana C. G., Bujanovic M., *Energies*, **2014**, *7*, 857 – 873

13. Mao J. Z., Zhang L. M., Xu F., *Cellul. Chem. Technol.*, **2012**, *46*, 193 – 205

14. Norgren M., Edlund H., Wagberg L., *Langmuir*, **2002**, *18*, 2859 – 2865

15. Deng Y., Feng X., Zhou M., Qian Y., Yu H., Qiu X., *Bio Macromol.*, **2011**, *12*, 1116 – 1125

16. Crestini, C.; Melone, F.; Sette, M.; Saladino, R., *Biomacromolecules*, **2011**, 12, 3928

17. Sarkanen S., Teller D. C., Stevens C. R., McCarthy J. L., *Macromol.*, **1984**, *17*, 2588 – 2597

18. Cheng G., Kent M. S., He L., Varanasi P., Dibble D., Arora R., Deng K., Hong K., Melnicheko Y. B., Simmons B. A., Sing S., *Langmuir*, **2012**, *28*, 11850 – 11857

19. Petridis L., Pingali S. V., Urban V., Heller W. T., Neill H. M., Foston M., Ragauskas A., Smith J. C., *Phys. Rev. E.*, **2011**, *83*, 061911-1

20. Harton S. E., Pingali S. V., Nunnery G. A., Baker D. A., Walker S. H., Muddiman D. C., Koga T., Rials T. G., Urban V. S., Langan P., *ACS Macro Lett.*, **2012**, *1*, 568 – 573

21. Lindstrom, T., *Colloid Polym. Sci.*, **1979**, *257*, 277

22. Contreras S., Gaspar A. R. Guerra A., Lucia L. A., Argyropoulos D. S., *Biomacromolecules*, **2008**, *9*, 3362–3369

23. Baker DA, Rials TG, Recent advances in low-cost carbon fiber manufacture from lignin. *Journal of Applied Polymer Science*, 2013, 130: 713-728.

24. J. Dealy, R. Larson, Structure and Rheology of Molten Polymers, Hanser publication, (2006)

25. Gao C., Qian H., Wang S., Yan D., Chen W., Yu G., *Polymer*, **2003**, 44, 1547–1552

26. Ramzi A., Prager M., Richter D., Efstratiadis V., Hadjichristidis N., Young R. N., Allgaier J. B., *Macromolecules*, 1997, **30**, 7171-7182

27. Larue I., Adam M., Zhulina E. B., Rubinstein M., Pitsikalis M., Hadjichristidis N., Ivanov D. A., Gearba R. I., Anokhin D. V., Sheiko S. S., *Macromolecules*, 2008, **41**, 6555-6563.

28. Bang J., Viswanathan K., Lodge T. P., Park M. J., Char K., *Journal of Chemical Physics*, 2004, **121**, 11489-11500

29. Rubinstein M.; Colby R. H.; Oxford University Press, **2003**.

30. Saito T. Perkins JH, Vautard F, Meyer HM, Messman JM, Tolnai B, Naskar AK. Methanol Fractionation of Softwood Kraft Lignin: Impact to the Lignin Properties, *ChemSusChem* 7(1), 221-228 (2014).

31. Saito T, Perkins JH, Jackson DC, Trammel NE, Hunt MA, Naskar AK. Development of lignin-based polyurethane thermoplastics, *RSC Advances* 3(44), 21832-21840 (2013).

32. Delmas G-H, Benjelloun-Mlayah B, Bigot Y L, Delmas M. Functionality of Wheat Straw Lignin Extracted in Organic Acid Media, *Journal of Applied Polymer Science*, 121, 491–501 (2011).

33. Beaucage G., *J. Appl. Cryst.*, 1996, *29*, 134-146.

34. Guinier, A. and G. Fournet, "Small-Angle Scattering of X-Rays", John Wiley and Sons, New York, **1955**

35. Daoud M., Cotton J. P., *J. Physique*, **1982**, *43*, 531 – 538

36. Delmas G-H, Benjelloun-Mlayah B, Bigot Y L, Delmas M. Biolignin Based Epoxy Resins, J. Appl. Polym. Sci. 127: 1863–1872, 2013

37. Sluiter, A.; Crocker, D.; Hames, B.; Ruiz, R.; Scarlata, C.; Sluiter, J.; Templeton, D. National Renewable Energy Laboratory Technical Report on "Determination of Structural Carbohydrates and Lignin in Biomass". NREL/TP-510-42618. 2008. (http://www.nrel.gov/biomass/pdfs/42618.pdf)

38. Sykes, R.; Kodrzycki, B.; Tuskan, G.; Foutz, K.; Davis, M. Within tree variability of lignin composition in Populus. *Wood Sci Technol*. **2008**, 42, 649-661.

39. Izumi, A.; Kurada, K. Pyrolysis-mass spectrometry analysis of dehydrogenation lignin polymers with various syringly/guaiacyl ratios. Rapid Communication in Mass Spectrometry 11: 1709-1715, 1997.